

The YORP effect with finite thermal conductivity

D. Čapek, D. Vokrouhlický*

Institute of Astronomy, Charles University, Prague, V Holešovičkách 2, CZ-18000 Prague 8, Czech Republic

Received 5 May 2004; revised 4 July 2004

Available online 25 September 2004

Abstract

The Yarkovsky–O’Keefe–Radzievskii–Paddack (YORP) effect has been recently suggested to significantly change, on a long-term, rotation state of small asteroids and meteoroids. Though YORP is closely related to the Yarkovsky (orbital) effect, it differs from the latter in two aspects: (i) YORP needs bodies of irregular shape to be effective, and (ii) YORP acts on bodies of zero surface thermal conductivity. To simplify computations, YORP has been so far investigated in the zero surface thermal conductivity limit only. Here we analyze the role of the surface conductivity and we find it substantially changes previous conclusions. Most importantly, unlike in the zero-conductivity limit, (i) YORP preferentially tilts obliquity toward two asymptotic states perpendicular to the orbital plane, and (ii) YORP asymptotically decelerates and accelerates rotation rate in about equal number of cases. Our work also indicates that direct detection of the YORP effect for a small asteroid may significantly constrain its mass.

© 2004 Elsevier Inc. All rights reserved.

Keywords: Asteroids; rotation; Meteoroids; YORP effect

1. Introduction

The Yarkovsky–O’Keefe–Radzievskii–Paddack (YORP) effect is a radiation torque due to thermally re-emitted sunlight by cosmic bodies (Rubincam, 2000; Vokrouhlický and Čapek, 2002). On a long-term, YORP can significantly change rotation rate and obliquity of small bodies in the Solar System, driving them toward some asymptotic values. Together, and sometimes in concert, with the related Yarkovsky effect, YORP may represent a key element to explain several puzzling facts about rotational, orbital and physical parameters of small asteroids and meteoroids (Rubincam, 2000; Rubincam et al., 2002; Vokrouhlický and Čapek, 2002; Bottke et al., 2003; Morbidelli and Vokrouhlický, 2003; Vokrouhlický et al., 2003). YORP can be also directly detected through a measurable change in phase of the sidereal rotation of small asteroids (Vokrouhlický et al., 2004a).

These applications require an accurate determination of the YORP effect strength for a given object or a class of objects, a task which is often uneasy because of the intrinsic YORP dependence on its/their detailed shape. The only simplification, as regards to the Yarkovsky effect, is that YORP does not need finite surface thermal conductivity to operate and can be estimated in the (unrealistic) limit of zero conductivity. To our knowledge, previous literature (Rubincam, 2000; Vokrouhlický and Čapek, 2002) adopted this simplifying assumption, mainly to allow faster computation, and at best arbitrary fudge factors have been introduced to account for finite surface conductivity.

In this paper, a follow-up of Vokrouhlický and Čapek (2002), we compute the YORP effect for various individual bodies, and also a large, statistical sample of synthetic bodies, and we account for a finite value of the surface thermal conductivity using a full-fledged thermal model. We find the conclusions of the simplified, zero-conductivity model change both quantitatively and qualitatively. An important specific result concerns ability of YORP to accelerate or decelerate asteroid’s rotation rate. By proving that the relevant YORP component depends weakly on surface conductivity

* Corresponding author. Fax: +420-2-2191-2567.
E-mail address: vokrouhl@mbox.cesnet.cz (D. Vokrouhlický).

value, we show here that the YORP detection constrains asteroid's mass more tightly than analogous detection of the Yarkovsky effect (Chesley et al., 2003).

2. Theory

We start with a brief comment on the YORP theory. A common basis of the Yarkovsky and the YORP effects is a recoil force $d\mathbf{f}$, applied to an oriented surface element $d\mathbf{S}$, due to thermal re-emission of the absorbed sunlight. With the simplifying assumption of Lambert (isotropic) surface emission we have (Spitale and Greenberg, 2001; Bottke et al., 2003)

$$d\mathbf{f} = -\frac{2}{3} \frac{\varepsilon \sigma T^4}{c} d\mathbf{S}, \quad (1)$$

where ε is the thermal emissivity, σ the Stefan–Boltzmann constant, T the surface temperature and c the light velocity. Integrating over the whole surface, one obtains the resulting thermal torque

$$\mathbf{T} = \int \mathbf{r} \times d\mathbf{f}. \quad (2)$$

In practice, we describe irregular shapes using the polyhedral model (see, e.g., Simonelli et al., 1993; Dobrovolskis, 1996; Vokrouhlický and Čapek, 2002), with surface composed of a finite number of triangular facets; fine-resolution models, e.g., Asteroids 1998 KY26, Golevka, Ida or Eros in Section 3, have a couple thousands to tens of thousands elements, while Gaussian spheres in Section 4 are transformed into 1004-facet polyhedrons.¹ The integration (2) is performed as a sum over the triangular surface elements.

Assuming the body rotates around the shortest axis of the inertia tensor (with the moment of inertia C), the main simplification adopted in this paper, we have $\mathbf{L} = C\omega \mathbf{e}$ for the angular momentum of the body; ω is the angular velocity of rotation and \mathbf{e} is the unit vector of the spin axis. The rate of change of \mathbf{L} in the inertial frame is equal to the applied torque \mathbf{T} : $d\mathbf{L}/dt = \mathbf{T}$. For $C = \text{const.}$ this equation splits into

$$\frac{d\omega}{dt} = \frac{\mathbf{T} \cdot \mathbf{e}}{C} \equiv \frac{T_s}{C}, \quad (3)$$

$$\frac{d\mathbf{e}}{dt} = \frac{\mathbf{T} - (\mathbf{T} \cdot \mathbf{e}) \mathbf{e}}{C\omega}. \quad (4)$$

It is useful to parametrize the spin vector \mathbf{e} with the obliquity ϵ , the angle between \mathbf{e} and normal vector \mathbf{N} to the orbital plane, and the precession in longitude ψ , such that \mathbf{e} decomposition into orbital plane unit vectors (x -coordinate along the nodal line) reads: $(\sin \epsilon \sin(\psi + \Omega), \sin \epsilon \cos(\psi + \Omega), \cos \epsilon)$, where Ω is the longitude of ascending node (see

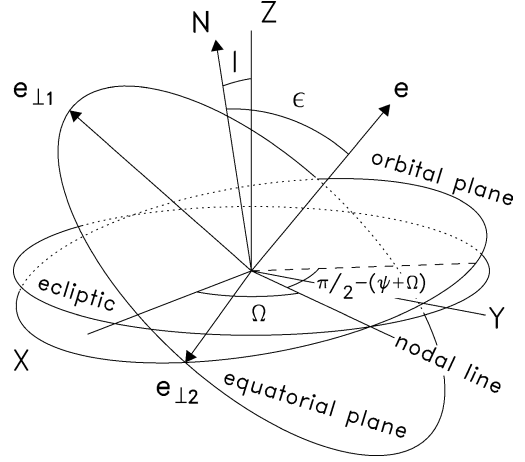


Fig. 1. Vectors and angular parameters introduced in the text; the XYZ reference frame is that of ecliptic of a fixed date, to which the moving orbital plane of date is inclined by I (and the nodal line offset by Ω from the X direction). Spin axis of the asteroid is along the unitary vector \mathbf{e} , and the asteroid equatorial plane of date defines auxiliary vectors $\mathbf{e}_{\perp 1}$ and $\mathbf{e}_{\perp 2}$. Obliquity ϵ is the angle between normal vector \mathbf{N} to the orbital plane and the spin vector \mathbf{e} . The angular distance of \mathbf{e} 's projection onto the orbital plane and nodal line is equal $\pi/2 - (\psi + \Omega)$.

Fig. 1 for various vectorial and angular variables defined). Then (4) yields

$$\frac{d\epsilon}{dt} = \frac{\mathbf{T} \cdot \mathbf{e}_{\perp 1}}{C\omega} \equiv \frac{T_\epsilon}{C\omega}, \quad (5)$$

$$\frac{d\psi}{dt} = \frac{\mathbf{T} \cdot \mathbf{e}_{\perp 2}}{C\omega} \equiv \frac{T_\psi}{C\omega}, \quad (6)$$

with the unit vectors

$$\mathbf{e}_{\perp 1} = \frac{(\mathbf{N} \cdot \mathbf{e}) \mathbf{e} - \mathbf{N}}{\sin \epsilon}, \quad (7)$$

$$\mathbf{e}_{\perp 2} = \frac{\mathbf{e} \times \mathbf{N}}{\sin \epsilon}. \quad (8)$$

In reality \mathbf{T} includes, aside to the YORP torque (2), additional contributions such as the gravitational torque due to the primary and/or inertial terms due to the motion of the orbital frame to which the angles ϵ and ψ are referred (e.g., Vokrouhlický and Čapek, 2002). The gravitational and inertial terms generally prevail in the precession component T_ψ , so that the corresponding YORP contribution is negligible and will not be discussed below. On the other hand, their long-term value in T_s and T_ϵ is nil, while YORP produces non-zero secular effects in the rotation speed and obliquity. We thus focus here on these two components of the thermal torque. Since the major effects of the YORP torque act on long time scales, we always assume T_s and T_ϵ averaged over rotation and revolution cycles. We assume no commensurability between rotation and orbital motion. As a simplification, we also assume circular orbit of the body around the primary which implies that T_s and T_ϵ depend on the obliquity only. Our method can be easily used for eccentric orbits too, but for discussion in this paper it would mean further extension of the parameter space. Focusing on the

¹ Our experience shows this number of surface facets makes the YORP strength computation accurate to several up to ten percents in the worst cases; this does not corrupt out statistical conclusions.

role of the surface conductivity, we thus stay with circular orbits.

The major unknown quantity in (1) is the surface temperature T that depends on external sources of energy (such as the incident solar radiation and body's reflectivity in the optical band expressed by the albedo coefficient A), and the way how the absorbed energy is conducted into deeper layers in the body. The latter is the heat diffusion problem (HDP) with appropriate boundary conditions and depends on various thermal constants, primarily thermal conductivity. To avoid necessity of solving HDP, one can, in the crudest approximation, assume a limit of zero thermal conductivity in which thermal radiation is emitted with no time lag; then $\varepsilon\sigma T^4 \approx (1 - A)\Phi(\mathbf{n} \cdot \mathbf{n}_0)$, where Φ is the solar radiation flux impinging on the surface element with exterior normal vector \mathbf{n} along direction \mathbf{n}_0 (Rubincam, 2000; Vokrouhlický and Čapek, 2002). Rubincam (2000) proposed to account for the effects of the finite thermal conductivity by using a scaling (“fudge”) factor $2/3$, but we shall see below that this is far too simplified approach.

The main purpose of this paper is to remove the approximation of zero-thermal conductivity and compute YORP for its realistic values. To that end we need to solve HDP, a sufficiently difficult task for a body of irregular shape. The problem may be however reasonably simplified, and still stay fully appropriate for most Solar System applications, when penetration depth of the thermal phenomena is much smaller than the geometric size of the body.² In this case, the fully three-dimensional HDP solution is not necessary and one-dimensional model accounting only for depth under a surface element is sufficient. We adopt this approach and solve HDP for each of the surface elements independently calculating temperature T depending on depth z and time t . The heat diffusion equation thus reads

$$\rho C \frac{\partial T}{\partial t} = K \frac{\partial^2 T}{\partial z^2}, \quad (9)$$

where ρ is the density, C is the specific heat capacity and K is the thermal conductivity.³ Appropriate boundary conditions, notably (i) energy input on the surface, (ii) constancy of the temperature at large depth, and (iii) periodicity of the solution over the rotation and revolution cycles are taken into account. The first two read

$$\varepsilon\sigma T^4(t, 0) = K \frac{\partial T}{\partial z}(t, 0) + E(t), \quad (10)$$

$$\frac{\partial T}{\partial z}(t, \infty) = 0, \quad (11)$$

² Note the penetration depth of the seasonal thermal wave in solid rocks is a few meters for typical asteroidal distances from the Sun; the diurnal thermal wave penetrates to a depth smaller by at least an order of magnitude. Our results are thus safely applicable for asteroids larger than tens of meters across.

³ These physical constants should be understood as effective values in the surface slab with thickness of several penetration depths of the seasonal thermal wave.

where we explicitly made clear the boundary position in depth z . Here $E = (1 - A)\Phi(\mathbf{n} \cdot \mathbf{n}_0)$ is the radiative energy flux. The “no-boundary” condition in time is best expressed using the orbital mean anomaly ℓ instead of t , so that $T(\ell, z)$ is constructed 2π -periodic in ℓ . Standard discretization method is used to represent the heat diffusion equation (9) (e.g., Press et al., 1994) and Spencer et al. (1989) scheme is used for the non-linear surface boundary condition (10). The surface energy input function $E(t)$ is computed from the known position of the Sun with respect to the surface element which is a function of the chosen orbit and the rotation pole of the asteroid. We also take into account a possibility of mutual shadowing on the surface. The “isothermal-core” condition (11) is applied at typically 10–15 penetration depths of the seasonal thermal wave. Practice shows that an isothermal initial seed in the whole mesh converges to the desired solution fast enough, so that we stop iterations of the numerical solution when a fractional change in temperature of all surface elements between two successive iterations is smaller than 0.001.

With the procedure outlined above, we obtain temperature T for each of the surface facets at any time along the orbit around the Sun. This value is used in Eq. (1) to compute the corresponding radiative recoil force differential.

3. YORP dependence on surface conductivity: individual cases

In this section we illustrate the role of thermal conductivity for YORP determination in the case of four asteroids whose shape is accurately known from either spacecraft reconnaissance or radar ranging analysis. Though their shapes will be accounted for, the orbits are all assumed circular and at $a = 2.5$ AU distance from the Sun (we note that the YORP torques scale as $\propto 1/a^2$ for circular orbits). In general, elliptic orbits are not considered here in order to demonstrate YORP dependence on the surface thermal conductivity without unnecessarily extending the free-parameter space. However, our method is straightforwardly applicable to specific bodies on elliptic orbits too (e.g., Vokrouhlický et al., 2004a). In what follows we provide accurate results for Golevka and Eros, in order to estimate a possibility of the YORP detection for these targets.

A general feature of the YORP-driven evolution is to tilt the axis toward a specific value of the obliquity. In accord with Rubincam (2000), Vokrouhlický and Čapek (2002) or Botke et al. (2003), we call this obliquity value asymptotic. While reaching this obliquity state, the YORP model adopted above predicts a permanent increase or decrease of the rotation period (see, however, comments in Section 5).

⁴ It also appears useful to scale depth z with the penetration depth h_T of the diurnal thermal wave, thus introduce $z' = z/h_T$; see Vokrouhlický and Farinella (1998).

3.1. Golevka

Shape models of both Golevka and 1998 KY26, available at <http://www.eecs.wsu.edu/~hudson/> as 4092-facet polyhedral figures, were obtained by analysis of radar ranging echoes in 1995 and 1998 (Hudson et al., 2000; Ostro et al., 1999). Both are small near-Earth asteroids on Apollo-type orbits; Golevka resides in the 3/1 mean motion resonance with Jupiter and close to the 4/1 exterior mean motion resonance with the Earth (that makes it now observable in close approaches with the Earth every 4 years during a couple decades). Both Golevka and 1998 KY26 were predicted to be good candidates for detection of the Yarkovsky effect (Vokrouhlický et al., 2000), and in the Golevka's case that detection has been already achieved (Chesley et al., 2003). Assuming a plausible bulk density of 2.5 g/cm^3 , Chesley et al. (2003) estimate surface thermal conductivity of $K \simeq 0.01 \text{ W/(mK)}$, also a likely value for the surface characterized as a mixture of dusty areas and exposed porous rocks (Hudson et al., 2000). Below we investigate dependence of the YORP effect strength on Golevka's surface conductivity for the simplest orbital configuration (circular orbit), and then provide accurate computation of the YORP effect for the real Golevka's orbital and spin parameters and the value of the surface conductivity inferred from the Yarkovsky effect detection.

Figure 2 shows mean rate of change of the angular velocity (left) and obliquity (right) due to YORP for a number of values of the surface conductivity K in the range 10^{-9} to 10 W/(mK) . Other surface thermal and physical parameters were: surface density 1.7 g/cm^3 , mean bulk density 2.5 g/cm^3 , specific heat capacity $C = 680 \text{ J/(kg K)}$ and albedo set to zero for simplicity. A striking conclusion from Fig. 2 is a near independence of the angular velocity YORP torque (T_s/C) on K , while in the same time a strong dependence of the obliquity YORP torque (T_e/C) on K . Zero, or very low conductivity YORP model would predict three pos-

sible asymptotic obliquity states 0° , 90° , and 180° (Type IV in Vokrouhlický and Čapek, 2002), while only a single asymptotic state— 90° —occurs for $K \geq 5 \times 10^{-5} \text{ W/(mK)}$.

The near independence of the rotation rate effect on K is important, see also other results below and discussion in Section 5, and warrants a comment. Equation (3) indicates that the rotation rate change is determined by the torque \mathbf{T} projection onto the rotation axis \mathbf{e} . As such, it basically depends on the amount of energy thermally reprocessed at a given latitude on the body. Thermal inertia (conductivity) affects delay with which the absorbed energy is re-emitted, but not the total amount of this energy; rotation cycle averaging, assumed in our procedure, then effaces differences between solutions corresponding to different values of surface thermal conductivity and explains our result. Note that the obliquity variation—Eq. (5)—depends on projection of \mathbf{T} onto $\mathbf{e}_{\perp 1}$ and thus breaks the symmetry. We only note that as the surface conductivity increases to large values the amplitude of the effect decreases as a response to more latitudinally uniform temperature distribution.

Next we determined YORP-induced evolution of the rotation period and sidereal rotation phase for Golevka using formulation by Vokrouhlický et al. (2004a). Thermal parameters as above, thermal conductivity $K = 0.01 \text{ W/(mK)}$ in accordance with Chesley et al. (2003), but here we consider the true orbital and spin parameters of the asteroid (e.g., Hudson et al., 2000). With that model we estimate the mean value of the fractional change of the rotation period P , $(dP/dt)/P \simeq -2.2 \times 10^{-7} \text{ yr}^{-1}$. This translates into a sidereal rotation phase change of $\simeq 70^\circ$ by 2010 and $\simeq 95^\circ$ by 2015, assuming origin in 1995 when a large international campaign was organized to determine Golevka's rotation state (Mottola et al., 1997). Unfortunately no photometry was recorded during the last decent close approach to the Earth in May 2003 and this means that the uncertainty interval of the sidereal phase, as follows from the 1995 data, is

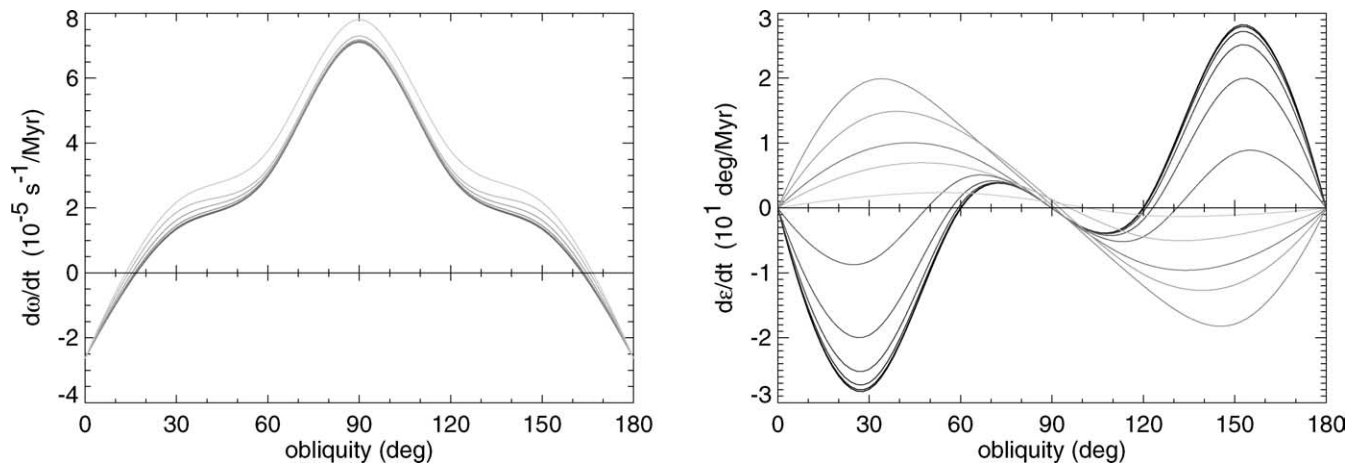


Fig. 2. YORP-induced mean rate of change of the rotation rate ω and obliquity ϵ as a function of the obliquity for Asteroid 6489 Golevka (a circular orbit at 2.5 AU assumed). Eleven values of the surface thermal conductivity $\log K = -9, -8, \dots, -1, 0, 1$ are shown in the decreasing scale of grey (the result for the lowest value—black—is identical to the zero-conductivity case analyzed by Vokrouhlický and Čapek, 2002). The rotation effect shows small dependence on K , while the obliquity effect depends on K significantly.

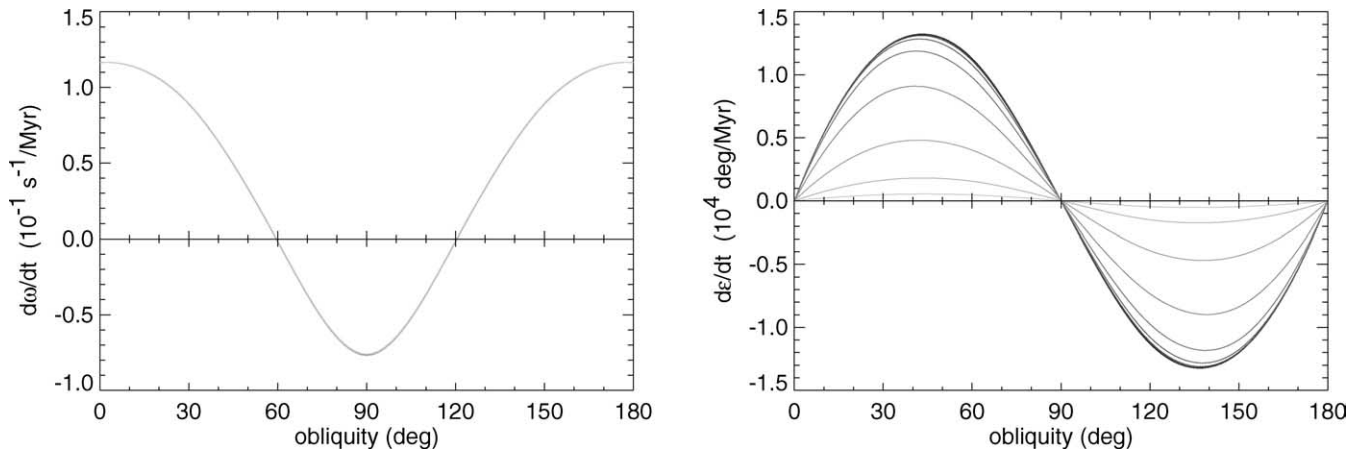


Fig. 3. The same as in Fig. 2 but for Asteroid 1998 KY26.

larger than the YORP signal up until $\simeq 2020$. We did not investigate in detail whether analysis of the radar echoes from May 2003 (and those from June 1991) could help to significantly reduce the phase uncertainty. The next observation possibilities occur in October/November 2007, 2011, 2015, and 2019, but the object fades from $\simeq 20.4$ to $\simeq 22.3$ mean visible magnitude. Given the rather large effect, and reliably well known shape of Golevka, we deem to think that a combined analysis of the available data and from those future apparitions might have a power to reveal existence of the YORP effect on this target. This appears interesting since in combination with the Yarkovsky measurement (Chesley et al., 2003) the bulk and surface parameters of this asteroid might be better constrained.

3.2. 1998 KY26

This is an unusual case of a very small asteroid whose fortuitously close encounter with the Earth in June 1998 allowed a detailed radar and photometric observations (Ostro et al., 1999). Analysis of the radar data allowed shape reconstruction, but rotation pole remains uncertain (though probably far from the ecliptic plane; P. Pravec, private communication). Little is also known about the physical properties (narrow-band photometry color indexes and radar polarization data slightly preferring C-type classification), but the small size and the fast rotation suggest a dust-free surface with likely a higher conductivity value.

1998 KY26's small size gives fewer chances to observe the target than it is usual; luckily the orbit has been secured by optical astrometry taken in February 2002 (Tholen, 2003) and fairly good prospects are to observe in September 2013, when the asteroid becomes a $\simeq 23.4$ magnitude object, and especially in June 2024 during the next decent⁵ close approach to the Earth. Vokrouhlický et al. (2000) predicted that by that time the Yarkovsky effect should be easily detected

for this asteroid, and Vokrouhlický and Čapek (2002) noticed that the YORP effect should be revealed too (using the zero-conductivity model). Here we substantiate the second of these predictions by using a thermal model and YORP computation that takes into account a finite value of the surface conductivity.

Figure 3 shows mean rate of change of the angular velocity (left) and obliquity (right) due to YORP for the surface conductivity K values in the same range as above for Golevka. We again note near-independence of the rotation rate effect on K , and a strong dependence of the obliquity effect on K . In this case, the increasing value of K decreases strength of the obliquity effect without modifying its asymptotic values.

If our result is scaled to the pericenter distance of $\simeq 1$ AU we confirm that YORP should fractionally change sidereal rotation period of this asteroid in June 2024 by $\simeq (1 - 2) \times 10^{-3}$, a comfortably large value to be detected.⁶ However, already the 2013 apparition of 1998 KY26 may represent a first possibility to directly detect the YORP effect for this target. The September observations, with a large ($\simeq 3$ -m) telescope, might by themselves reveal the effect since the affordable synodic rotation period uncertainty in a two-week period observation run could be $\leq 10^{-4}$ (fractionally). By that time, the expected fractional change of the sidereal rotation period due to the YORP effect should be $\simeq (5 - 10) \times 10^{-4}$. Moreover observation during the April 2013 opposition could yield data at entirely different phase than in 1998, helping thus to constrain pole orientation (and thus determining transformation between the synodic and sidereal rotation periods). We note the 2024 encounter is closer to the Earth, but does not yield a possibility of such a larger phase coverage as the 2013 apparition.

⁶ The same result might be also obtained for a very small target 2004 FH, for which P. Pravec and his group measured the synodic rotation period of $\simeq 3.02$ min with a fractional error of $\simeq 1.6 \times 10^{-4}$ in March 2004. This asteroid gets in a close approach in January 2018, and with even a smaller size than 1998 KY26, notably $D \simeq 20$ m, we may expect the YORP change of the rotation period is safely larger than the uncertainty level in 2004.

⁵ On June 1, 2024 the asteroid distance from the Earth becomes $\simeq 0.03$ AU, smaller than any other value till 2099.

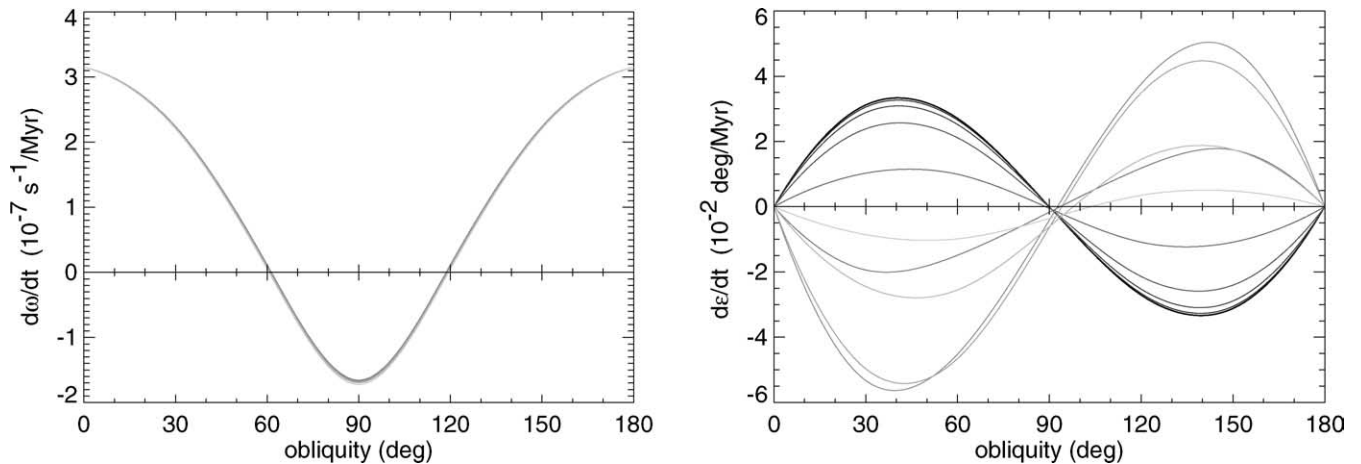


Fig. 4. The same as in Fig. 2 but for Asteroid 433 Eros.

3.3. Eros

From the multitude of the Eros shape models in the post-NEAR era (e.g., Miller et al., 2002; Konopliv et al., 2002), we use the 7790 facet representation downloaded from the PDS node <http://pdssbn.astro.umd.edu>. This is a convenient compromise between satisfactory accuracy and yet reasonable computer time expenses to solve HDP for each of the surface elements along one revolution about the Sun.

The mean YORP-induced variations of the Eros-shaped object on a circular orbit at 2.5 AU distance from the Sun are shown at Fig. 4. We again conclude near-independence of the rotation rate effect on the value of surface conductivity K , while significant dependence of the obliquity effect on that parameter. In particular, for $K \simeq 5 \times 10^{-4}$ W/(m K) the asymptotic obliquity values become 0° and 180° , while for lower conductivities was 90° (in Section 4 we find this behavior typical for high-conductivity situation). Interestingly, this 5×10^{-4} W/(m K) threshold value is near the plausible one that Eros might have had when it was residing in the main asteroid belt. This might suggest that the characteristic YORP timespan to modify initial obliquity was perhaps long, comparable or longer than the Solar System age. On the other hand, the characteristic YORP timespan to modify rotation rate is of the order of $\simeq 750$ Myr. This information is interesting after Vokrouhlický et al. (2004, work in preparation) have found Eros rotation state unusual and speculate about its implication about past orbital (and rotational) evolution of this asteroid.

To check a possibility of the YORP detection we computed the corresponding orbit-averaged torque components for the actual Eros' orbit and its spin state (e.g., Miller et al., 2002). We used surface conductivity $K \simeq 0.005$ W/(m K), specific heat capacity $C = 680$ J/(kg K), surface and bulk densities of 2 and 2.67 g/cm³, respectively corresponding to predominantly powdered regolith (e.g., Morrison, 1976; Harris and Davies, 1999; Sullivan et al., 2003). With those

parameters we obtained the mean fractional change of Eros' rotation period $(dP/dt)/P \simeq 1.4 \times 10^{-9}$ yr⁻¹.

Eros is the largest near-Earth asteroid so it is not surprising that detection of the YORP effect, despite of very accurate NEAR/Shoemaker data, is unlikely. With results above, we estimate that the sidereal rotation phase change due to YORP at around 1900 was $\simeq 4^\circ$, more than an order of magnitude smaller than would be necessary.⁷ Eros is obviously easily observable target, but we estimate that YORP would be discernible only after decades. Yet, it might have sense to record Eros lightcurve in the future (enough once every decade) as a low priority, long-term project for detection of the YORP effect at this target; amateur astronomers might perhaps be interested in this effort.

3.4. Ida

The shape of Ida, $2^\circ \times 2^\circ$ latitude–longitude grid model constructed from Galileo images (Thomas et al., 1996), has been obtained from the PDS node <http://pdssbn.astro.umd.edu> and transformed to the appropriately dense polyhedral model. Figure 5 shows mean rate of change of the angular velocity and obliquity due to YORP for different values of the surface conductivity for this body. As expected from the work of Vokrouhlický et al. (2003), YORP drives obliquity toward its extreme values (0° or 180°) while decelerating its rotation rate. The characteristic YORP timescale, such as to double its rotation rate, is $\simeq 2$ Gy in a very good agreement with Vokrouhlický et al.'s model. The only surprising element is the asymptotic deceleration of Ida's rotation rate, since its rotation period of $\simeq 4.63$ hr is comparatively fast. Formation event of the small moon Dactyl might have recently perturbed Ida's rotation, but without more constraints we cannot resolve this problem.

⁷ We thank J. Āurech for having shown us his careful analysis of early Eros photometric data from the beginning of 20th century prior publication.

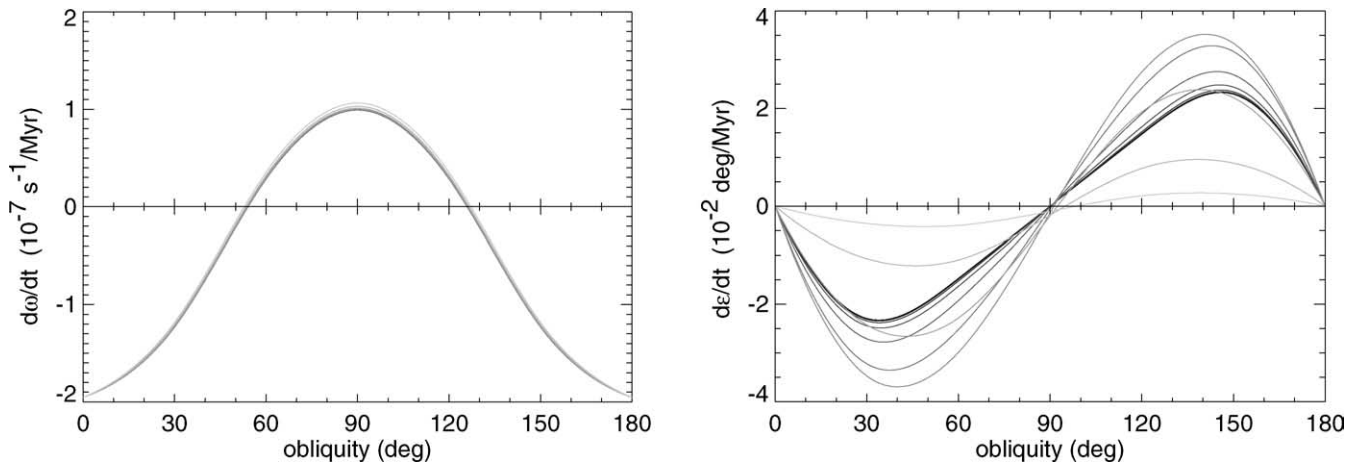


Fig. 5. The same as in Fig. 2 but for Asteroid 243 Ida.

4. YORP dependence on surface conductivity: statistical analysis

Above we dealt with individual bodies, for which spacecraft or radar observations allowed detailed shape reconstruction. There is, however, only a limited number of such cases and we need additional sample of plausible asteroid-shape objects that could serve to derive statistical characterization of YORP. To date, the best suited technique introduced by Muinonen (1998), and Muinonen and Lagerros (1998), uses Gaussian random spheres to construct a large set of shapes in an automated way. Parameters of the Gaussian random spheres used in this paper are those of Muinonen and Lagerros (1998) fitted to a limited sample of small main-belt asteroids. Similar bodies have been already used by Vokrouhlický and Čapek (2002) to characterize statistical properties of YORP in the zero conductivity limit.

In what follows we considered a sample of 200 Gaussian random spheres normalized to have the same volume, equal to a sphere with a radius of 1 km. All bodies were assumed to revolve about the Sun on a circular orbit with semimajor axis of 2.5 AU. Mean bulk and surface densities were 2.5 g/cm^3 , surface heat capacity 680 J/(kg K) and albedo set to zero for simplicity. Surface thermal conductivity varied from 0.001 W/(m K) , appropriate for highly particulate, regolith-type surface, to 0.01 W/(m K) , appropriate to a mixture of particulate and stony surface. For comparison we also performed simulations with zero surface conductivity using the technique of Vokrouhlický and Čapek (2002). Higher values of conductivity were not investigated in this study, partly because of large CPU expenses and partly because high-conductivity surfaces are less likely for small, kilometer-size inner-main-belt asteroids (compatible with S spectral classes; e.g., Harris and Lagerros, 2003). For sake of definiteness we assumed 6 hr rotation period when reporting mean values of the obliquity change, but these results may be easily re-scaled to an arbitrary value of rotation period using Eq. (5).

Figure 6 shows orbit-averaged rate of change of the rotation rate (right part) and obliquity (left part) due to YORP effect in the zero-conductivity limit. We note about the same likelihood of asymptotically approaching 0° (or 180°) and 90° obliquity. Comparison of bottom and top panels, where we separated the solutions with different asymptotic obliquity values, indicate that in majority of the cases rotation becomes asymptotically decelerated (see also Fig. 11 in Vokrouhlický and Čapek, 2002). A typical timescale to evolve the rotation state, e.g., double the rotation period or significantly change the obliquity, is about 15 Myr for our test objects (see also Fig. 9).

Figures 7 and 8 show the same quantities as in the Fig. 6, but here the surface conductivity K was 0.001 and 0.01 W/(m K) , respectively. As expected from results in Section 3, the rotation rate variation $d\omega/dt$ is little modified by the finite value of the surface conductivity, while the rate $d\epsilon/dt$ by which obliquity changes due to YORP depends significantly on the K value. Most importantly, as the conductivity increases, majority of bodies are asymptotically driven to 0° (or 180°) obliquity; for instance this happens in 95% of the cases for $K = 0.01 \text{ W/(m K)}$. Because the rotation rate torque did not change much, this result also implies that YORP with finite surface conductivity nearly equally accelerates and decelerates bodies rotation. These conclusions are in sharp contradiction with those from the zero-conductivity model, indicating that the value of the surface conductivity significantly influences statistical properties of the way how YORP modifies rotation of small bodies.

Another perspective to see these results is given in Fig. 9 to 11 where characteristic strength of both YORP torques— T_s/C and T_ϵ/C —is compared for the three surface conductivity cases: $K = 0 \text{ W/(m K)}$ (Fig. 9), $K = 0.001 \text{ W/(m K)}$ (Fig. 10), and $K = 0.01 \text{ W/(m K)}$ (Fig. 11). The left panels of these figures show characteristic timescale to double nominal rotation period of 6 hr by YORP at the asymptotic obliquity value binned in 5 Myr cells, while the right panels show maximum value of the obliquity rate $d\epsilon/dt$ due to YORP binned in 2.5 deg/Myr cells. Median values, roughly

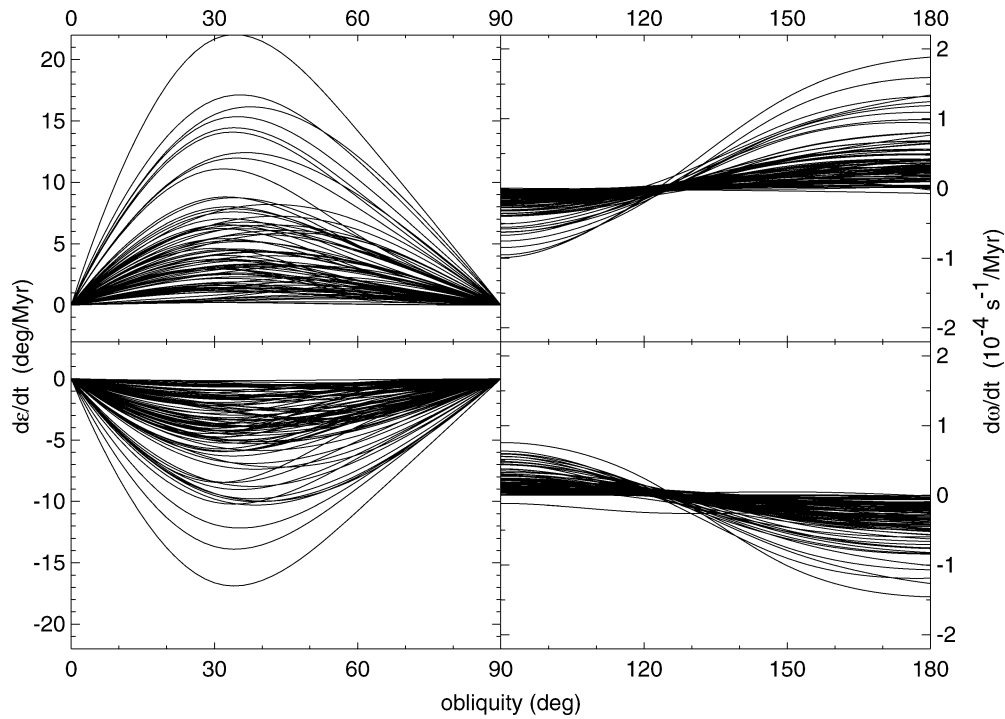


Fig. 6. Estimated mean rate of change of the rotation frequency (right parts) and the obliquity (left parts) due to the YORP effect as a function of obliquity. A sample of 200 Gaussian random spheres used, all normalized to have a volume of a sphere with a radius of 1 km and rotation period of 6 hr; the obliquity rate is proportional to the assumed rotation period. Results here assume zero surface thermal conductivity. We note $d\omega/dt$ is symmetric in the complementary obliquity interval, while $d\epsilon/dt$ is antisymmetric under this transformation (see discussion in Vokrouhlický and Čapek, 2002). For clarity, we separate solutions whose asymptotic obliquity value is 90° (upper panels), from those whose asymptotic obliquity value is 0° (180° ; bottom panels). In this way we note that there is approximately equal number of cases for each of the asymptotic obliquity values, while most of the cases—95%—asymptotically decelerate rotation rate.

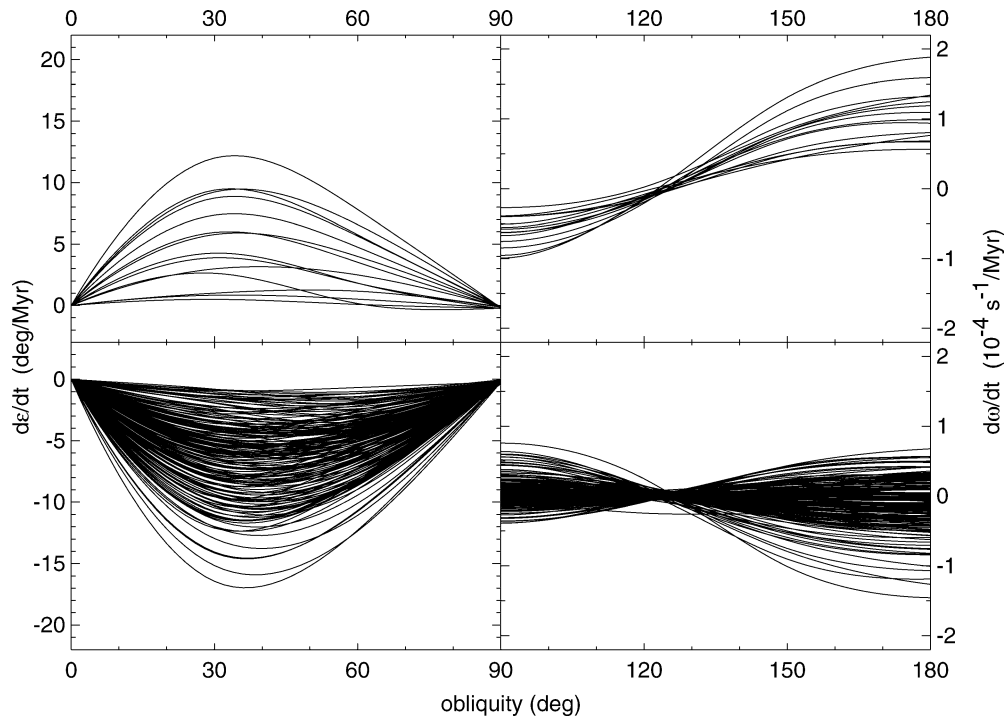


Fig. 7. The same as in Fig. 6 but now a surface thermal conductivity of 10^{-3} W/(m K) assumed. Here about 80% of cases is driven toward the asymptotic obliquity values of 0° or 180° , and about 40% of objects asymptotically accelerate rotation rate.

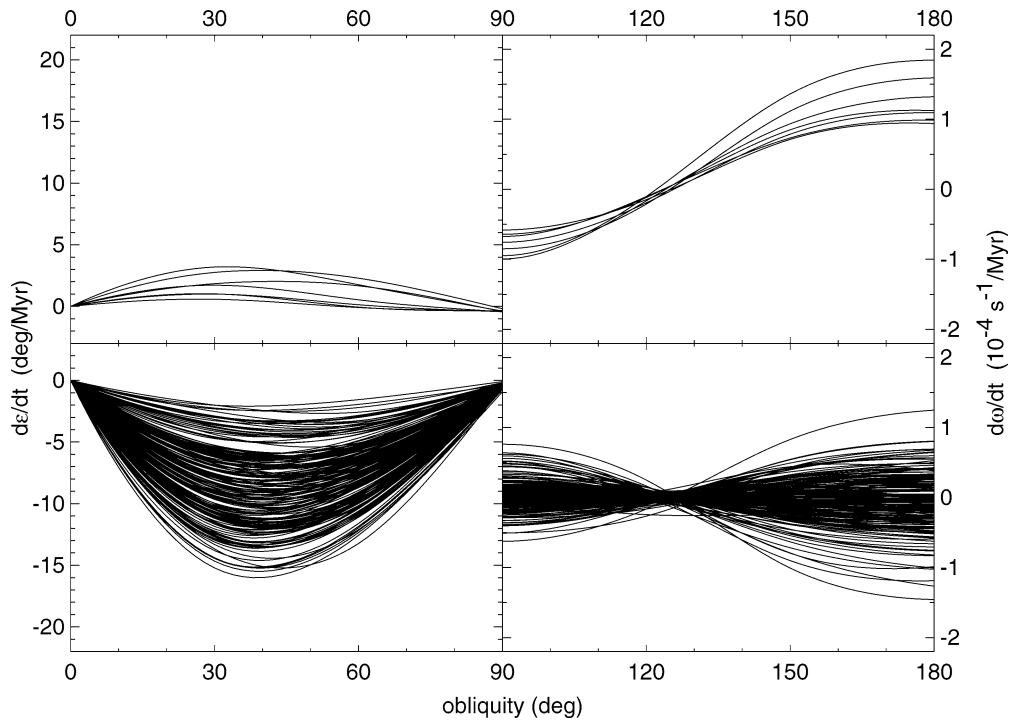


Fig. 8. The same as in Fig. 6 but now a surface thermal conductivity of 10^{-2} W/(mK) assumed. Here about 95% of cases is driven toward the asymptotic obliquity values of 0° or 180° , and about equal number of bodies asymptotically accelerate and decelerate rotation rate.

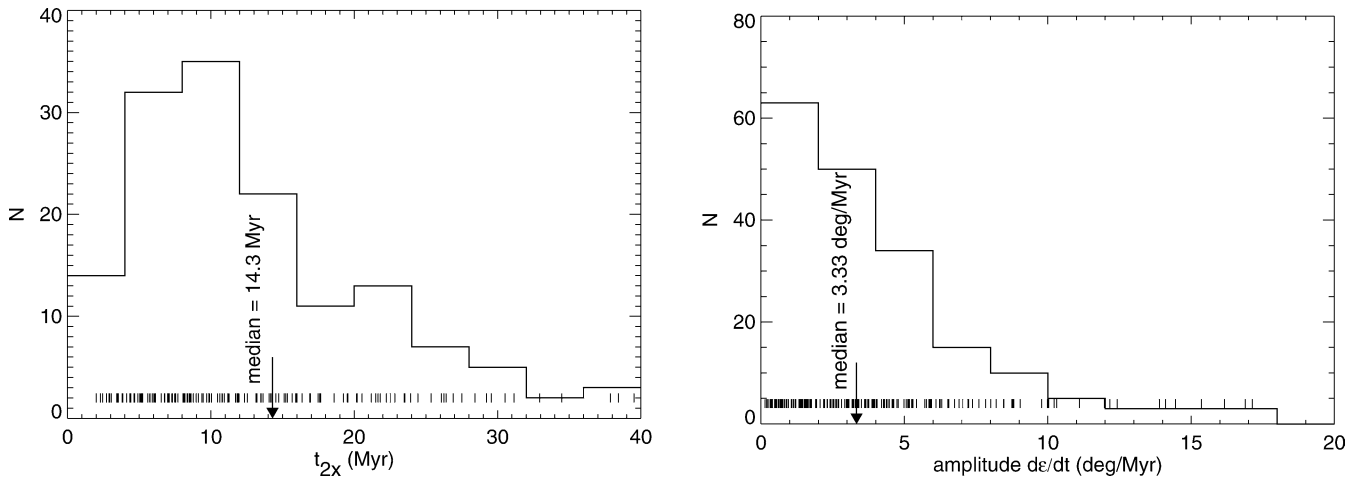


Fig. 9. Statistical occurrence of the characteristic timescale to double rotation period at the asymptotic obliquity value (left) and maximum obliquity rate (right) over a sample of Gaussian random spheres. Small bars at bottom indicate the actual values and the arrow shows median values. These results assume bodies with volume equivalent to a sphere of 1 km radius and rotation period of 6 hr; the doubling-timespan scales inversely proportionally, while the obliquity rate proportionally to the assumed rotation period. Zero surface thermal conductivity for all bodies.

10–15 Myr and a couple deg/Myr, are also indicated. While the rotation rate characteristics are similar for all values of the surface conductivity K , the obliquity variation strength increases as K increases.

5. Discussion and conclusions

Finite (non-zero) value of the surface conductivity is not necessary for YORP to operate, but here we proved that it

significantly affects YORP component tilting spin axis with respect the orbital plane, while leaving unaffected the component accelerating or decelerating rotation rate. Using a large sample of Gaussian random spheres, believed to represent shape of small main-belt asteroids, we determined that for vast majority of bodies YORP drives spin axis to become perpendicular to the orbital plane. In the same time, rotation rate may appear accelerated or decelerated with about equal probability. Both these results are novel and in contradiction with conclusions from zero surface conductivity model.

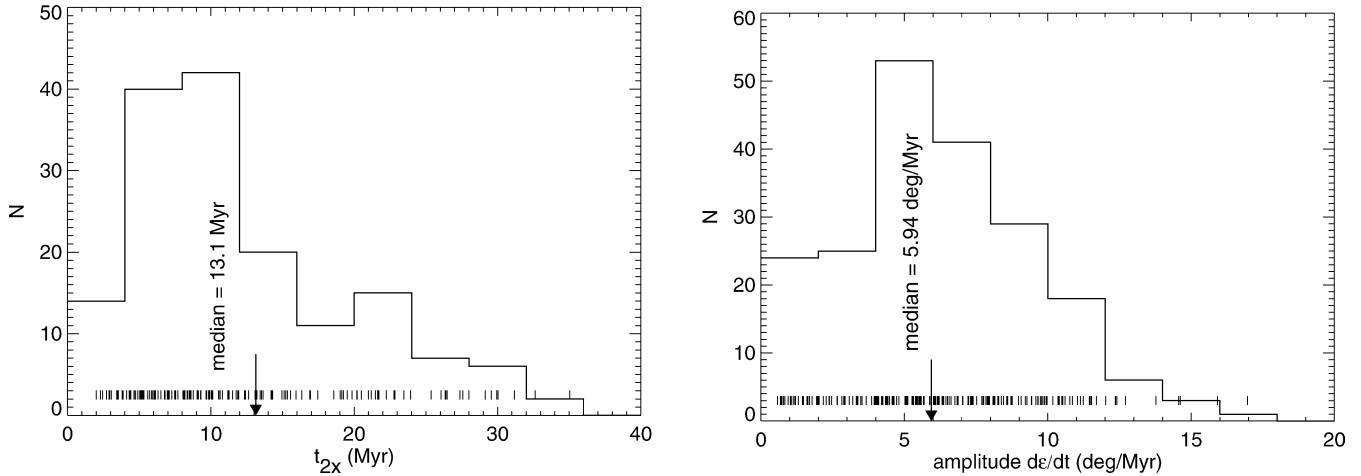


Fig. 10. The same as in Fig. 9 but here for a surface thermal conductivity of 10^{-3} W/(mK). While the median doubling timespan shortens, the median obliquity rate increases.

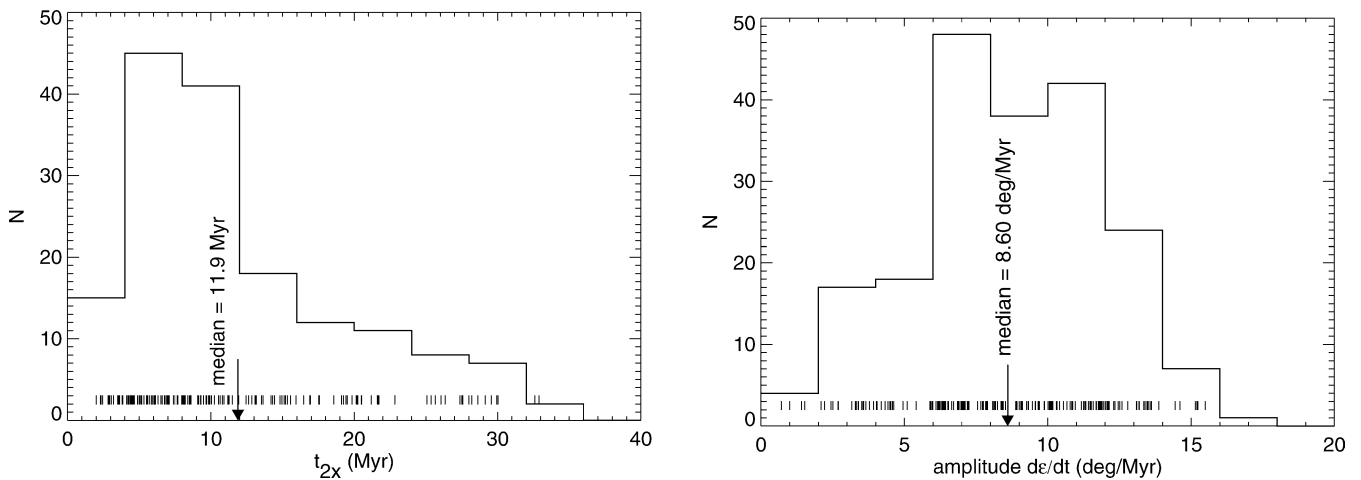


Fig. 11. The same as in Fig. 9 but here for a surface thermal conductivity of 10^{-2} W/(mK). While the median doubling timespan shortens, the median obliquity rate increases.

Results of [Vokrouhlický et al. \(2003\)](#) are in accordance with these conclusions, because their model explaining anomalous distribution of spin axis orientation and rotation rates of Koronis asteroids requires preferential evolution of the obliquity toward its extreme values. Another hint may come from a slightly preferential overall orientations of asteroid rotation axes toward poles of the ecliptic (e.g., [Pravec et al., 2003](#); [La Spina et al., 2004](#)). However, before drawing more detailed conclusions we need to account, aside to YORP, for additional important effects such as secular spin-orbit resonances or mutual asteroid collisions.

[Vokrouhlický et al. \(2004b\)](#) have recently suggested that several detections of the Yarkovsky effect every year are likely during the next decade. The YORP detection possibilities (e.g., [Vokrouhlický et al., 2004a](#)) will be also searched, and certainly rapidly increase in number in the next years. Here we investigated YORP discovery possibilities for Golevka, 1998 KY26 and Eros, and found (or confirmed) very good prospect for 1998 KY26 and perhaps Golevka. Moreover, a discovery of a very weak dependence

of the relevant YORP torque on the surface conductivity is important in general because it suggests the YORP detections might constrain asteroid's mass independently from its surface thermal conductivity. Obviously a caveat of such a YORP determination of asteroid's mass is the necessity to know its shape very precisely; so far only radar ranging or direct spacecraft reconnaissance meet the required level of accuracy. However, it also seems likely that good YORP detection candidates would also allow detection of the Yarkovsky effect (e.g., [Ostro et al., 2004](#)), and conjunction of both detections would fairly well constrain asteroid's mass and surface thermal properties in an uncorrelated way.

All previous studies of the YORP effect ([Rubincam, 2000](#); [Vokrouhlický and Čapek, 2002](#)), including this paper, assumed principal axis rotation and rigid shape of the body. These assumptions are well satisfied for “normal rotators” (rotation periods of several hours, say) but fail for slow rotators ([Pravec et al., 2004](#)) or very fast rotators ([Pravec et al., 2003](#)). Not only the current YORP models cannot be applied to these extreme cases, but more importantly, by making the

bodies to evolve toward fast and slow rotators, YORP makes a generic link between normal and extreme rotators. What exactly happens along this evolutionary path cannot be determined with the limited YORP models today. For instance, YORP may despin rotation enough to trigger non-principal-axis rotation mode and become thus a natural mechanism to explain a class of tumbling asteroids (Pravec et al., 2004). In the opposite limit, YORP may steadily accelerate rotation rate of an asteroid until structural changes, and possibly even fission, occur; this would make YORP an interesting candidate mechanism for creating binary systems. Further YORP-work needs to be directed along these generalizations of the current models.

Acknowledgments

This work has been supported by the Grant Agency of the Czech Republic, under the grant No. 205/02/0703. We also thank Observatory and Planetarium at Hradec Králové whose computer facility has been partly used. Suggestions from D. Nesvorný and D.P. Rubincam, as referees, helped to improve the original form of this paper.

References

- Bottke, W.F., Vokrouhlický, D., Rubincam, D.P., Brož, M., 2003. Dynamical evolution of asteroids and meteoroids using the Yarkovsky effect. In: Bottke, W.F., Cellino, A., Paolicchi, P., Binzel, R.P. (Eds.), *Asteroids III*. Univ. of Arizona Press, Tucson, pp. 395–408.
- Chesley, S.R., Ostro, S.J., Vokrouhlický, D., Čapek, D., Giorgini, J.D., Nolan, M.C., Margot, J.-L., Hine, A.A., Benner, L.A.M., Chamberlin, A.B., 2003. Direct detection of the Yarkovsky effect via radar ranging to near-Earth Asteroid 6489 Golevka. *Science* 302, 1739–1742.
- Dobrovolskis, A.R., 1996. Inertia of any polyhedron. *Icarus* 124, 698–704.
- Harris, A.W., Davies, J.K., 1999. Physical characteristics of near-Earth asteroids from thermal infrared spectrophotometry. *Icarus* 142, 464–475.
- Harris, A.W., Lagerros, J.S.V., 2003. Asteroids in the thermal infrared. In: Bottke, W.F., Cellino, A., Paolicchi, P., Binzel, R.P. (Eds.), *Asteroids III*. Univ. of Arizona Press, Tucson, pp. 205–218.
- Hudson, R.S., 26 colleagues, 2000. Radar observations and physical modeling of Asteroid 6489 Golevka. *Icarus* 148, 37–51.
- Konopliv, A.S., Miller, J.S., Owen, W.M., Yeomans, D.K., Giorgini, J.D., Garmier, R., Barriot, J.-P., 2002. A global solution for the gravity field, rotation, landmarks, and ephemeris of Eros. *Icarus* 160, 289–299.
- La Spina, A., Paolicchi, P., Kryszezińska, A., Pravec, P., 2004. Retrograde spins of near-Earth asteroids from the Yarkovsky effect. *Nature* 428, 400–401.
- Miller, J.K., 10 colleagues, 2002. Determination of shape, gravity, and rotational state of Asteroid 433 Eros. *Icarus* 155, 3–17.
- Morbidelli, A., Vokrouhlický, D., 2003. The Yarkovsky-driven origin of near Earth asteroids. *Icarus* 163, 120–134.
- Morrison, D., 1976. The diameter and thermal inertia of 433 Eros. *Icarus* 28, 125–132.
- Mottola, S., 28 colleagues, 1997. Physical model of near-Earth Asteroid 6489 Golevka (1991 JX) from optical and infrared observations. *Astron. J.* 114, 1234–1245.
- Muironen, K., 1998. Introducing the Gaussian shape hypothesis for asteroids and comets. *Astron. Astrophys.* 332, 1087–1098.
- Muironen, K., Lagerros, J.S.V., 1998. Inversion of shape statistics for small Solar System bodies. *Astron. Astrophys.* 333, 753–761.
- Ostro, S.J., 19 colleagues, 1999. Radar and optical observations of Asteroid 1998 KY26. *Science* 285, 557–559.
- Ostro, S.J., 15 colleagues, 2004. Radar observations of Asteroid 25143 Itokawa (1998 SF36). *Meteorit. Planet. Sci.* 39, 407–424.
- Pravec, P., Harris, A.W., Michałowski, T., 2003. Asteroid rotation. In: Bottke, W.F., Cellino, A., Paolicchi, P., Binzel, R.P. (Eds.), *Asteroids III*. Univ. of Arizona Press, Tucson, pp. 113–122.
- Pravec, P., 18 colleagues, 2004. Tumbling asteroids. *Icarus*. In press.
- Press, W.H., Flannery, B.P., Teukolsky, S.A., Vetterling, W.T., 1994. *Numerical Recipes*. Cambridge Univ. Press, Cambridge.
- Rubincam, D.P., 2000. Radiative spin-up and spin-down of small asteroids. *Icarus* 148, 2–11.
- Rubincam, D.P., Rowlands, D.D., Ray, R.D., 2002. Is Asteroid 951 Gaspra in a resonant obliquity state with its spin increasing due to YORP? *J. Geophys. Res.* 107 (E9), 5065.
- Simonelli, D.P., Thomas, P.C., Carcich, B.T., Veverka, J., 1993. The generation and use of numerical shape models for irregular Solar System objects. *Icarus* 103, 49–61.
- Spencer, J.R., Lebofsky, L.A., Sykes, M.V., 1989. Systematic biases in radiometric diameter determinations. *Icarus* 78, 337–354.
- Spitale, J., Greenberg, R., 2001. Numerical evaluation of the general Yarkovsky effect: effects on semimajor axis. *Icarus* 149, 222–234.
- Sullivan, R.J., Thomas, P.C., Murchie, S.L., Robinson, M.S., 2003. Asteroid geology from Galileo and NEAR Shoemaker data. In: Bottke, W.F., Cellino, A., Paolicchi, P., Binzel, R.P. (Eds.), *Asteroids III*. Univ. of Arizona Press, Tucson, pp. 331–350.
- Tholen, D.J., 2003. Recovery of 1998 KY26: implications for detecting the Yarkovsky effect. *Bull. Am. Astron. Soc.* 35, 972.
- Thomas, P.C., Belton, M.J.S., Carcich, B.T., Chapman, C.R., Davies, M.E., Sullivan, R., Veverka, J., 1996. The shape of Ida. *Icarus* 120, 20–32.
- Vokrouhlický, D., Čapek, D., 2002. YORP-induced long-term evolution of the spin state of small asteroids and meteoroids. Rubincam's approximation. *Icarus* 159, 449–467.
- Vokrouhlický, D., Farinella, P., 1998. The Yarkovsky seasonal effect on asteroidal fragments: a non-linearized theory for the plane-parallel case. *Astron. J.* 116, 2032–2041.
- Vokrouhlický, D., Milani, A., Chesley, S.R., 2000. Yarkovsky effect on small near-Earth asteroids: mathematical formulation and examples. *Icarus* 148, 118–138.
- Vokrouhlický, D., Nesvorný, D., Bottke, W.F., 2003. Thermal torques produce spin vector alignments among Koronis family asteroids. *Nature* 425, 147–152.
- Vokrouhlický, D., Čapek, D., Kaasalainen, M., Ostro, S.J., 2004a. Detectability of YORP rotational slowing of Asteroid 25143 Itokawa. *Astron. Astrophys.* 414, L21–L24.
- Vokrouhlický, D., Čapek, D., Chesley, S.R., Ostro, S.J., 2004b. Yarkovsky-detection opportunities. I. Solitary asteroids. *Icarus*. In press.